

Stabilisation of precipitates of pedogenic dissolved organic matter by multivalent cations

Daniela Gildemeister · George Metreveli · Sandra Spielvogel · Sabina Hens · Friederike Lang · Gabriele E. Schaumann

Received: 2 April 2014 / Accepted: 9 July 2014 / Published online: 30 July 2014
© Springer-Verlag Berlin Heidelberg 2014

Abstract

Purpose Precipitation of dissolved organic matter (DOM) by multivalent cations is important for biogeochemical cycling of organic carbon. We investigated to which extent cation bridges are involved in DOM precipitation and how cross-links by cations and water molecule bridges (WaMB) stabilise the matrix of precipitated DOM.

Materials and methods DOM was precipitated from the aqueous extract of a forest floor layer adding solutions of $\text{Ca}(\text{NO}_3)_2$, $\text{Al}(\text{NO}_3)_3$ and $\text{Pb}(\text{NO}_3)_2$ with different initial metal cation/C (Me/C) ratios. Precipitates were investigated by differential scanning calorimetry before and after ageing to detect

cation bridges, WaMB and restructuring of supramolecular structure.

Results and discussion Twenty-five to sixty-seven per cent of the dissolved organic carbon was precipitated. The precipitation efficiency of cations increased in the order $\text{Ca} < \text{Al} < \text{Pb}$, while the cation content of precipitates increased in the order $\text{Pb} < \text{Ca} < \text{Al}$. The different order and the decrease in the WaMB transition temperature (T^*) for $\text{Al/C} > 3$ is explained by additional formation of small AlOOH particles. Thermal analysis indicated WaMB and their disruption at T^* of 53–65 °C. Like cation content, T^* increased with increasing Me/C ratio and in the order $\text{Ca} < \text{Pb} < \text{Al}$ for low Me/C. This supports the general assumption that cross-linking ability increases in the order $\text{Ca} < \text{Pb} < \text{Al}$. The low T^* for high initial Me/C suggests less stable and less cross-linked precipitates than for low Me/C ratios.

Conclusions Our results suggest a very similar thermal behaviour of OM bound in precipitates compared with soil organic matter and confirms the relevance of WaMB in stabilisation of the supramolecular structure of cation-DOM precipitates. Thus, stabilisation of the supramolecular structure of the DOM precipitates is subjected to dynamics in soils.

Responsible editor: Dong-Mei Zhou

Electronic supplementary material The online version of this article (doi:10.1007/s11368-014-0946-9) contains supplementary material, which is available to authorized users.

D. Gildemeister · G. Metreveli · S. Hens · G. E. Schaumann (✉)
Institute for Environmental Sciences, Group of Environmental and Soil Chemistry, Universität Koblenz-Landau, Fortstr. 7,
76829 Landau, Germany
e-mail: schaumann@uni-landau.de

D. Gildemeister
Umweltbundesamt, FG IV 2.2 Pharmaceuticals, Wörlitzer Platz 1,
06844 Dessau-Roßlau, Germany

S. Spielvogel
Department of Geography, Institute of Integrated Natural Sciences,
Universität Koblenz-Landau, Universitätsstr. 1, 56070 Koblenz,
Germany

S. Hens
GN Dr. Netta; Beratende Ingenieure und Geowissenschaftler,
Bienengarten 3, 56072 Koblenz, Germany

F. Lang
Albert-Ludwigs-Universität Freiburg, Institute of Forest Sciences,
79085 Freiburg i.Br., Germany

Keywords Cation bridges · Cross-link · Differential scanning calorimetry · Dissolved organic matter · Glass transition · Water molecule bridges

1 Introduction

Precipitation of dissolved organic matter (DOM) by multivalent metal cations (e.g. Pb, aluminium (Al) and iron (Fe)) can play an important role in the biogeochemical cycling of organic carbon (OC) (Borggaard et al. 2005; Khare et al. 2005) especially in acidic forest soils, such as Podzols (Lang et al. 2005). These soils are characterised by substantial

stabilisation of OC via sorption and precipitation (Kalbitz and Kaiser 2008). The precipitated organic matter (OM) is more resistant against microbial decay if compared with the respective DOM solution (Scheel et al. 2007) as a consequence of decreased bioavailability (Scheel et al. 2008). Therefore, the loss of OC is reduced in soils with higher cation concentrations (Oste et al. 2002; Römken and Dolfing 1998; Shen 1999). Al precipitates are especially assumed to stabilise large amounts of OM (Mulder et al. 2001; Schwesig et al. 2003), but divalent cations like Pb^{2+} or Ca^{2+} can also bridge between negatively charged molecules of DOM (Klitzke et al. 2008; Lang et al. 2005), leading to the formation of precipitates of the cation and OM.

It is generally assumed that organic molecules and their segments can be cross-linked via cation bridges (Miikki et al. 1997; Piccolo 2002; Wershaw 2004). This is supported by molecular modelling studies (Aquino et al. 2011). Also, reduced solubility and mineralisation of OC in Ca-treated soils was at least partly ascribed to cation bridges (Baldock and Skjemstad 2000).

Such cation-OM interactions that result in a network structure of OM hold together by mediated cation cross-links may also increase the stability of metal-organic precipitates. Depending on the thermodynamic situation and on the spatial distribution of hydrophilic functional groups in OM, cation bridges can occur either via inner sphere complexes or via outer sphere complexes, such that the maximum distance required for cation bridges between two OM segments can be significantly increased by water molecule bridges (WaMB) (Kunhi Mouvenchery et al. 2013; Schaumann et al. 2013a, b). Despite its proposed relevance for various ecological functions of soil organic matter (SOM), until now, the cation bridge mechanism is still under discussion (Kunhi Mouvenchery et al. 2012).

One reason is the lack of methods suitable for characterisation of the heterogeneous natural organic matter (NOM), which are also capable to identify intermolecular linkages and distinguish them from intramolecular ones and to assess molecular and supramolecular rigidity of the NOM matrix. For a comprehensive discussion of methods, please refer to Kunhi Mouvenchery et al. (2012). In summary, X-ray absorption fine-structure spectroscopy (XAFS) and extended XAFS can give structural information on the environment of the cation of interest and its coordination geometry within 5 Å distance (Plaschke et al. 2004; Xia et al. 1997). They are, however, not capable for distinguishing multidentate organomineral complexes from intermolecular cross-links. Addressing NMR active nuclei like ^{27}Al , ^{23}Na or ^{25}Mg (Bardy et al. 2007), NMR spectroscopy also can provide information on the coordination environment of those cations. Advanced methods may even be able to assess the mobility of these nuclei and therefore obtain indirect information on the molecular rigidity of the OM environment. The major

difficulty is, however, the low natural abundance for most of the NMR active isotopes and interference with clay minerals, which is especially challenging for ^{27}Al NMR (Kunhi Mouvenchery et al. 2012). Recent methodical investigations show that ^1H NMR wideline analysis can be used to detect WaMB in soils (Jäger et al. 2011; Kunhi Mouvenchery et al. 2013; Schaumann and Bertmer 2008; Schaumann and Bertmer 2013; Schaumann et al. 2013a); however, it addresses rather the quantity of water molecules involved in WaMB than their effect on the rigidity of the supramolecular OM structure. Small angle X-ray scattering (SAXS) techniques provide information on intermolecular interactions caused by multivalent cations (Lang et al. 2005), yet are limited to dissolved or only very small particulate constituents.

One of the most suitable methods directly assessing matrix rigidity and, therefore changes in cross-linking status in NOM, is thermal analysis (Schaumann et al. 2013b), which allows detection of glass transitions if present (LeBoeuf and Weber 2000) or disruption of WaMB (Schaumann and Bertmer 2008; Schaumann and LeBoeuf 2005) upon heating. WaMB can occur either involved in cation bridges or as direct cross-linkers between hydrophilic functional groups (Kunhi Mouvenchery et al. 2012; Schaumann and Thiele-Bruhn 2011). They can increase matrix rigidity themselves, but their stability will also depend on the rigidity of the surrounding environments (Kunhi Mouvenchery et al. 2012), such that WaMB will be disrupted at higher temperature if the molecular surroundings of them are more rigid (Schaumann and Bertmer 2008; Schaumann and Thiele-Bruhn 2011). Thus, the higher the glass transition temperatures (T_g) or WaMB transition temperatures (T^*), respectively, the higher is the matrix rigidity. As cation bridges are expected to induce the rigidity of the matrix of the metal-organic precipitates, they are expected to increase T_g and/or T^* . Moreover, a cross-linked organic matrix within the precipitates would be amorphous and therefore subjected to continuous physical and physicochemical ageing processes (Schaumann 2005, 2006) during which matrix rigidity continuously increases.

The precipitation of DOM by multivalent cations at constant pH can have two central reasons: (1) reduction of repulsive forces between DOM molecules due to charge saturation of the negatively charged functional groups by the cations and/or (2) increase in apparent molecular size due to bridging between individual DOM molecules (Piccolo 2002; Wershaw 2004).

Besides the well-described cross-links via inner sphere and outer sphere complexes (Dudal et al. 2006; Lu and Allen 2002; Plaschke et al. 2010; Weng et al. 2002), DOM functional groups can also be bridged by combination of cation bridges and WaMB as shown recently for a sapric histosol sample (Kunhi Mouvenchery et al. 2013) and for the organic layer of a haplic podzol sample (Schaumann et al. 2013b). In these cases, larger clusters of water molecules can support the

bridging of larger distances between functional groups than required for direct cation bridges. Involvement of WaMB in cation bridges is highly relevant as it will lead to higher dynamics in SOM and in DOM precipitates. It is, therefore, essential to know to which extent classical cross-links, WaMB and cation bridges control matrix rigidity.

The objective of our study was to investigate, to which extent intermolecular cation bridges are responsible for the precipitation of DOM and how they stabilise the matrix of precipitated DOM. We hypothesised that, like for solid SOM, the supramolecular structure of air-dried DOM precipitates is stabilised by bridges of multivalent cations and that WaMB are involved in the stabilisation of the matrix of DOM precipitates. If cation bridges stabilise the precipitates, their matrix rigidity should increase with increasing cation valency and cation content. If WaMB are involved, we expect to observe WaMB transitions dependent on cation type and concentration and we expect that the transition temperatures increase upon ageing.

We investigated the effect of three multivalent cations on the thermal characteristics of cation-DOM precipitates exemplarily for the aqueous extract of the organic layer of a haplic podzol. In order to explore general principles on cation bridging, we used Ca^{2+} as the most abundant bivalent cation in the soil and two cations with stronger affinity to OM than Ca^{2+} but different valency. For this, we chose Al^{3+} and Pb^{2+} representing trivalent and bivalent cations, respectively. We created solutions with different cation/OC ratios, precipitated the DOM using nitrate salts of the multivalent cations Ca^{2+} , Pb^{2+} and Al^{3+} and conducted differential scanning calorimetry (DSC) measurements to study WaMB transitions and glass transitions in the precipitates.

2 Materials and methods

2.1 Sample preparation

The required DOC solution was obtained from the forest floor layer (Haplic Podzol; pH 3.7, SOC 430 mg g^{-1} , CEC_{eff} 303 $\text{mmol}_c\text{kg}^{-1}$) sampled in a forest stand dominated by 80-year-old Norway spruces (*Picea abies* L. [Karst.], Hohe Matzen, Fichtelgebirge) in South Germany. For basic characteristics of the forest floor sample, which was used for this study, see Schaumann et al. (2013b). Immediately after sampling, the material of the forest floor layer was homogenised, shock frozen with liquid nitrogen and stored in a freezer at -18°C . This procedure was chosen to produce DOM solutions from the forest floor sample with the same initial characteristics throughout the complete experimental study, independently of the duration of storage. As the OM in air-dried soils is subjected to continuous changes in matrix rigidity (Schaumann 2005; Schaumann et al. 2013b), the DOM release kinetics (Schaumann et al. 2000) and wettability (Diehl

et al. 2009) are substantially influenced by drying and drying methods. Thus, storage of an air-dried sample cannot ensure that DOM extracts from the air-dried forest floor sample will be the same irrespectively of the storage length.

For the experiments aliquots of the forest floor sample were unfrozen in a fridge and air dried. The water content of the aliquots differed between 7 and 8 % after drying. After drying, the aliquots were sieved to <1 mm and needles were removed manually.

2.2 Extraction of OM and preparation of DOC solution

OM was extracted with water from the forest floor in presence of an acid cation exchange resin to remove exchangeable cations from the organic and mineral soil constituents. With this procedure, the amount of DOM extractable from the forest floor sample was maximised with a specific focus on OM which had been immobilised in the forest floor sample by cations. One hundred grammes of the forest floor sample, 50 g of exchange resin (Amberlite[®], IR-120, H^+ Form) and 700 mL of deionised water were filled in a 1-L glass bottle (Duran[®]) and mixed overnight in an overhead shaker. Subsequently, the resin-soil solution was filtered over cellulose nitrate filters (Sartorius[®], pore size 0.45 μm) at a pressure of approximately 2 bar for 3 h, which had been rinsed prior to that with moderately warm water to reduce DOC losses of the filter material.

The total OC concentration of the obtained DOC solution was determined by TOC analysis (TOC Analyser Multi C/N 2100, Analytik Jena) and diluted with deionised water to an average concentration of 130 mg OC L^{-1} in the DOC-stock solution. This solution was further diluted to get an initial concentration of 9.8 mmol OC L^{-1} for the experiments (see next section). The obtained DOC solution was used immediately after extraction for the experiments to prevent changes caused by microbial activity and to avoid conservation methods that might have an influence on the sample characteristics.

2.3 Precipitation experiments

Different solutions of the nitrate salts of Ca, Pb and Al, varying in their Me^{n+} concentration, were prepared, in order to finally obtain Me/C ratios between 0.1 and 10 in the precipitation solution (Table 1). Nitrate salts were chosen due to the low solubility of PbCl_2 ($L=2\times 10^{-5}$ mol L^{-1}). For precipitation, 10 mL of the salt solution and 90 mL of the DOC solution were mixed in 100 mL glass bottles (Duran[®]) and sealed with PTFE-coated PBT screw caps. Additionally to the Me/C containing solutions, a control sample containing 10 mL deionised water and 90 mL DOC solution was prepared. Each precipitation experiment was conducted in duplicate.

Table 1 Me/C ratios in the precipitation solution obtained from preliminary experiments exploring the lowest concentration where flocculation occurred up to a maximum ratio of 10

Aluminium		Lead		Calcium	
Al/C (mol mol ⁻¹)	Initial Al _{total} (mmol L ⁻¹)	Pb/C (mol mol ⁻¹)	Initial Pb _{total} (mmol L ⁻¹)	Ca/C (mol mol ⁻¹)	Initial Ca _{total} (mmol L ⁻¹)
0.1	1	0.1	1	0.5	5
0.5	5	0.5	5	1	10
1	10	1	10	2	20
2	20	3	30	3	30
5	50	5	50	5	50
10	100	10	100	10	100

In contrast to the Al- and Pb-containing samples, visible flocculation for the Ca containing samples was only observed above a Me/C ratio of 0.5. Pb concentrations in contaminated soils like shooting range soils were reported up to 990 mg L⁻¹ (Cao et al. 2003), corresponding to 5 mmol L⁻¹. The higher Pb concentrations of this study were included for reasons of process research in order to cover the complete concentration range in which DOM precipitation by Pb was relevant

After shaking the samples for 5 min by hand, the pH value was measured and adjusted to 3.5 using 0.5, 1 or 2 M NaOH or 0.3 % HNO₃. The pH of the obtained solutions before adjustment ranged between 2.9 and 3.6. Subsequently to pH adjustment, the solutions were shaken over night in an overhead shaker and stored in an incubator at 5 °C for another night to minimise microbial utilisation. After 15–17 h of equilibration, the solutions were filtered at a pore size of 0.45 µm (Sartorius® Vaccum Filtration) with a rinsed cellulose nitrate filter at top and a glass fibre filter beneath (Whatman®, GF 6, Ø 47 mm) to improve the filtration flux. The filters were rinsed before filtration with moderately warm deionised water to prevent contaminations.

2.4 Chemical analyses of the filtrate solution

Immediately after filtration, the filtrates were analysed for their pH and their DOC concentration. Concentration of DOC was analysed using a TOC Analyser Multi C/N 2100 (Analytik Jena) after acidification and out gassing of inorganic carbon.

To calculate the loss of cations from the solution and to calculate the cation content in the precipitates, the cation concentration in the solutions was analysed. Therefore, an aliquot of each solution was diluted in a ratio of 1:1 with 10 % HNO₃ to enable conservation and storage of the solutions. The Ca concentration of the solutions was analysed using a Flame AAS (Perkin Elmer 4100) with an oxygen/acetylene flame and a wavelength of 422.7 nm, Al concentration was determined using a nitrous oxygen/acetylene flame (Varian AA 240 FS) with a wavelength of 308.2 nm, and Pb was analysed using a Graphite Tube AAS (Perkin Elmer 4100) with the furnace programme given in Table S1 of the Electronic supplementary material (ESM) and a wavelength of 283.3 nm.

The formation of dissolved complexes between metal cations and DOM was modelled for different Me/C ratios using a species calculation programme (Gustaffson 2010). The model description and details regarding input parameters are given in the SI.

2.5 Sample preparation and DSC measurements of the precipitates

After filtration, the precipitates were carefully removed from the surface of the cellulose nitrate filters using a spatula and directly filled into standard Al pans. It was intended to produce as many filled pans as possible from the precipitates to obtain the maximum possible number of replicates. The amount of precipitate was limited especially for the low Meⁿ⁺/C ratios.

All samples were dried for 4–5 days at 25 °C in the open DSC pans in an oven. By weighing the pans before and after the drying procedure, the water content of the wet samples was calculated. After weighing, the open pans were stored in a dessicator over silica gel and conditioned for 14 days. The dried precipitates were carefully pound with a spatula to assure a consistent heat transfer between pan and sample. The Al pans were then hermetically sealed and then investigated by DSC as described further below.

Two types of transitions have been discussed to be observed during DSC measurements of NOM: (i) the “classical” glass transition that also occurs in synthetic polymer systems and which is reversing through subsequent heating runs and (ii) a transition that can only be observed in closed systems and which is only slowly reversible after days or weeks of storage, depending on the sample (Schaumann 2005). The latter transition is due to the breakdown of WaMB between OM segments, and is consequently named “WaMB transition” (Schaumann et al. 2013b). The corresponding transition temperature “T*” will be referred to as “WaMB transition

temperature” to clearly distinguish between this specific thermal event and classical glass transitions. It is not possible to measure both events with one DSC procedure. Thus, after a first characterisation of the samples in measurement 1, part of the samples was measured by measurement 2 and the other part was investigated by measurement 3. For these follow-up measurements, always three replicates with well pronounced WaMB transitions from measurement 1 were chosen. As not enough replicates were available for conducting measurements 2 and 3, the samples were distributed between these measurements as indicated below.

All DSC measurements were conducted in standard Al pans using a DSC Q1000 (TA Instruments, Germany) with a refrigerated cooling system (RCS) and nitrogen as a purge gas. Temperature calibration was conducted using indium as standard.

Measurement 1 (all samples) was conducted in hermetically closed pans to characterise WaMB transitions (three to eight replicates depending on the amount of precipitate): abrupt cooling to $-50\text{ }^{\circ}\text{C}$ and subsequent heating with 10 K min^{-1} from -50 to $110\text{ }^{\circ}\text{C}$, followed by a second abrupt cooling and subsequent heating cycle.

Measurement 2 (samples with a molar Me/C ratio of 0.1, 1, 5 and 10; the latter only for Ca) was performed in open pans to characterise (polymer-like) glass transitions over the whole concentration range. For this, 14 days after measurement 1, three small holes ($\varnothing 1\text{ mm}$) were drilled in the lids of three replicate pans of the selected samples. Subsequently, the samples were weighed, dried overnight at $105\text{ }^{\circ}\text{C}$ to remove all water and weighed again to calculate the water loss of the samples. Then the DSC measurements were conducted. They started with a heating step of $105\text{ }^{\circ}\text{C}$ for 30 min to ensure complete water removal from the samples, followed by the same cooling and heating cycles as described for measurement 1. The test for classical glass transitions needed to be conducted in the whole concentration range. As measurement 2 is destructive, samples could not be used anymore for measurement 3. Therefore, precipitates of the intermediate Me/C ratios of 2 and 3 for all cations and 10 for Pb and Al were not investigated with measurement 2, but with measurement 3.

Measurement 3 (samples with a Me/C ratio of 2, 3 and 10; the latter only for Al and Pb) was performed in hermetic pans to test for the presence of ageing processes as it is typical for WaMB transitions (Schaumann et al. 2013b): Three replicate pans of the selected samples that had shown a clearly pronounced and mathematically analysable step transition during measurement 1 were measured again after 6 and 8 weeks of isothermal storage at $20\text{ }^{\circ}\text{C}$. Here, the pans remained hermetically sealed and the measurement procedure was consistent with the procedure described for measurement 1.

All DSC data were analysed using Universal Analysis version 4.1 (TA Instruments). Baseline correction was performed

using TZero technology[®] by TA Instruments. Where thermal events were less pronounced, which was the case for the Ca-DOM precipitates, the received heat flow curve was corrected by rotation prior to the determination of T^* , which corresponds to the subtraction of a linear baseline with the slope of the thermogram at temperatures below the transition; see Fig. S3 (ESM). By this correction method, the heat capacity of the sample changes, however, the transition temperature remains the same. The transition temperature T is indicated by an inflection point in the thermogram. Operationally, three tangent lines were applied for its evaluation and the corresponding transition temperature (T_g , T^*) was determined from the inflection point between the tangent lines. Since T^* corresponds to a non-reversing thermal event, we will concentrate on the first heating cycle in the following chapters.

3 Results and discussion

3.1 Precipitation efficiency and composition of the Me-DOM precipitates

Cation-induced precipitation of DOM differed significantly among the three cations. The precipitation and sedimentation process proceeded strongly and within minutes for Al and Pb, resulting in a clear supernatant. By contrast, Ca addition led to visible precipitates only at Me/C ratios above 0.5 (Table 1), and sedimentation was incomplete even after 15–17 h of equilibration. This was the first indication for significant differences in Me-DOM interactions between Ca on the one hand, and Pb and Al, on the other hand. These visual observations are confirmed by the DOC losses from solution obtained for the different Me/C mixtures (Fig. 1a).

The unprecipitated DOC content decreased from 90 to 80 mg L^{-1} (Ca) and from 62 to 40 mg L^{-1} (Pb) with increasing initial Me/C ratio, indicating precipitation of 25–32 and 48–67 % of the initial DOC for Ca and Pb, respectively. By contrast, the addition of Al^{3+} resulted in a re-increase of unprecipitated DOC for Me/C ratios above 2; i.e. addition of excess of Al re-increases solubility of OM. Al was able to precipitate 38 % (for Al/C=0.1 and 10) up to 50 % (for Al/C=5) of the initial DOC (Fig. 1a). For most Me/C ratios, the amount of precipitated DOM increased in the following order: $\text{Ca} < \text{Al} < \text{Pb}$. Similar tendency was observed for dissolved Me-DOM complexes by species calculations (Table S3, ESM); e.g. at Me/C ratio of 0.1, the total amount of metals complexed with functional groups of DOM was 0.3, 5.1 and 17.8 % for Ca, Al and Pb, respectively. The amount of carboxylic and phenolic functional groups complexed with metals increased in the same order (Table S4, ESM). The formation of dissolved complexes between metal cations and DOM can be considered as an initial step for further formation of Me-DOM

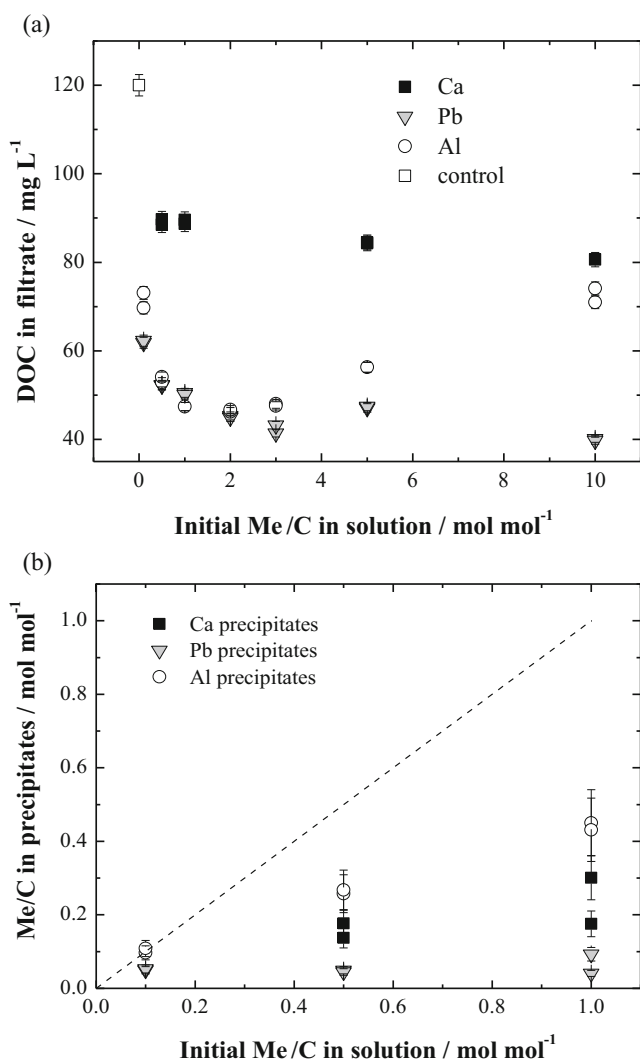


Fig. 1 **a** DOC content of the solutions after precipitation with Ca^{2+} , Pb^{2+} and Al^{3+} and of the control solution using different initial Me/C ratios. For the control, deionised water was used instead of salt solution. **b** Me/C ratio in precipitates for the three lowest Me/C ratios in initial solutions. Dashed line represents the 1:1 line. Error bars represent the standard deviation of individual measurements

precipitates. Furthermore, the species calculations showed for all Al/C ratios an oversaturation regarding to the Al oxyhydroxide (AlOOH). The oversaturation increased with increased Al/C ratio. In contrast to this, no oversaturation was observed for Ca and Pb containing samples. Species calculation with the consideration of precipitation would lead to maximum values for the fraction of Al precipitated as AlOOH ranging from 42 % for Al/C=0.1 to 97 % for Al/C=5. Since the species calculation is based solely on thermodynamic data and the kinetic processes like precipitation kinetics and diffusion are not considered but expected in our experiments, the formation of dissolved complexes between metal cations and DOM molecules was calculated in this contribution without allowing precipitation in oversaturated solutions. Since the precipitation of AlOOH is

thermodynamically possible, the formation of solid AlOOH particles in the real samples and within the real time span of the experiment cannot be fully excluded especially at high Me/C ratios. Due to the precipitation of AlOOH a lower amount of free Al^{3+} was obviously available for the formation of Me-DOM precipitates at high Me/C ratios. This can lead to a re-increase of unprecipitated DOC as it was observed in experiments with Al containing samples (Al/C ratios above 2).

The DOC losses caused by precipitation for Al/C ratios up to 0.5 in the initial solution, clearly exceeded those observed by Scheel et al. (2007). In contrast to the procedure in our study, Scheel et al. (2007) prepared the DOM solution by dissolution in distilled water, but without cation exchange resin. Thus, in that study, mainly that OM was dissolved, which was not retained in hardly soluble cation-OM complexes. In our study, the DOM solution was prepared in the presence of cation exchange resin, which removed large part of these cations, resulting in a mobilisation of the OM previously bound to them. It is obvious that especially this OM is re-precipitated again when interacting with the cations in the DOM precipitation solution. Consequently, the DOM in our study reveals a stronger precipitation efficiency than that extracted by Scheel et al. (2007).

The cation content of the Me-DOM precipitates (Fig. 1b) increased with increasing initial Me/C ratio. Out of all Me-DOM precipitates, the Al-DOM and the Pb-DOM precipitates revealed the highest and lowest Me/C ratio, respectively. The Me/C ratios in Me-DOM precipitates were generally lower than the Me/C ratios in initial solutions, indicating that only a part of cations were involved in the formation of precipitates. The high content of Al determined for Al-DOM precipitates can be an effect of formation of solid AlOOH particles and the filtration method used for sample treatment. If AlOOH particles are formed, they can be removed from the liquid phase together with Al-DOM precipitates by filtration. This can lead to the overestimation of the Al content in Al-DOM precipitates.

For Pb the calculated metal fraction bound in dissolved Pb-DOM complexes, including metals accumulated in diffuse double layer, are comparable to the metal fraction in Pb-DOM precipitates determined experimentally (Fig. S1, ESM). This indicates that by transition from dissolved complexes to the precipitates the Pb content does not change significantly for this metal. In contrast to this, for Ca and Al, a higher fraction of cations was observed in Me-DOM precipitates compared with dissolved complexes. Differences were especially distinct for Al also by considering a possible overestimation.

Water content in the wet precipitates was lower for Ca precipitates (16 ± 4 ; w/w) than for Al and Pb precipitates (23 ± 10 and 23 ± 5 , respectively), which suggests a lower hydrophilicity of Ca precipitates (Table S5, ESM). This effect tends to be higher for low Me/C ratios than for high Me/C ratios, but this trend was not significant. This could point to a decreasing hydrophilicity of the precipitates with increasing Me/C ratio. Also, water contents of

the precipitates after drying at 25 °C differed among cation type and initial Me/C ratio (Table S5, ESM). Whereas the dried Ca and Pb precipitates had water contents between 6 and 7 %, water contents of Al precipitates were considerably higher, ranging between 12 and 19 %, suggesting a higher hygroscopicity of the Al-DOM precipitates.

3.2 Thermal properties of Me-DOM precipitates

3.2.1 Assessment of transitions

Figure S2 (ESM) shows a typical representant for DSC thermograms for the first and second heating cycles of the air-dried precipitates. While the thermogram of the first heating cycle reveals a strongly pronounced step transition for each precipitate, the second heating cycle did not show any thermal events. The step transition of the first heating cycle was strongest pronounced in samples with the highest OM content. Step transition temperatures varied between 53 and 65 °C, and thus are in the range of those found for several peat and organic layer samples in previous studies (Hurraß and Schaumann 2006; Kunhi Mouvenchery et al. 2013; Schaumann et al. 2013b; Schaumann and LeBoeuf 2005). According to the criteria given by Schaumann and LeBoeuf (2005) and Schaumann and Bertmer (2008), these non-reversing transitions can be interpreted as WaMB transitions characterised by the WaMB transition temperature T^* .

T^* was less pronounced for Ca-DOM precipitates than for Pb-DOM and Al-DOM precipitates. Al precipitates showed similar curve shapes as the other precipitates and revealed the highest T^* values among all samples. The lack of additional thermal transitions supports the assumption that the potentially

co-precipitated AlOOH does not interfere in the regarded temperature range. In average, T^* increased up to 65 ± 3 °C with increasing initial Al/C solution ratio for Al/C ratios up to 3 and decreased again to 60 ± 1 °C for higher Al/C ratios (Fig. 2; DSC thermograms: Fig. S4, ESM). By contrast, T^* of the Pb-DOM-precipitates varied between 55 and 65 °C but showed no clear trend with increasing Pb/C ratio of the initial solution. Only for initial solution with a Pb/C ratio of 10, T^* was lower in comparison to the other ratios. Also for Ca-DOM-precipitates with initial Ca/C ratio of 5 and 10, lower T^* can be observed. In summary, precipitation with Al resulted in samples with distinctly higher matrix rigidity for most of the initial Me/C ratios followed by precipitation with Pb and Ca. This is in line with the general assumption that, among all cations investigated here, Al is the best cross-linking agent due to its higher charge and Pb most probably is a better cross-linking agent compared with Ca because of its high molecular mass.

Referring to the results presented above, two main topics will be discussed in the following: (1) The occurrence of a WaMB transition instead of a reversible glass transition during the first heating cycle of the DSC measurements of the precipitates and hence the role of water in the samples; (2) The increase and decrease of T^* depending on the Me/C ratio in the precipitates.

Figure 3 exemplarily shows thermograms for an air-dried Al-DOM precipitate before and after complete removal of water. No analysable thermal events occur in the thermogram of the water-free Al precipitate. This was observed for the thermograms of all water-free precipitates independently of the kind of cation involved in precipitation and irrespective of the Me/C ratio of the initial solution. These results—in combination with the clear dependence of T^* on the type of cation, demonstrate that there should be an interaction between water bridging and cations and it can be concluded that cation bridging itself induces no signals in DSC at the measured temperature ranges. Direct cation-OM interactions without involvement of water cannot be excluded. Their direct confirmation would require further investigations using EXAFS for confirmation of the identity of the next neighbours of cations. This additional question was beyond the scope of this study as we focused on the effect of multivalent cations on matrix rigidity.

Step transitions that can only be observed in closed systems and which are only slowly reversible after days or weeks of storage, are due to the breakdown of WaMB between SOM segments (Schaumann and Bertmer 2008; Schaumann and LeBoeuf 2005). Since all precipitates contained measureable amounts of water, the observed WaMB transitions are likely due to the disruption of WaMB among the SOM segments of the air-dried precipitates. This assumption is supported by the higher T^* observed for the Al precipitates containing more water compared with the WaMB transition temperatures of the Ca and Pb precipitates which contained less water and is in

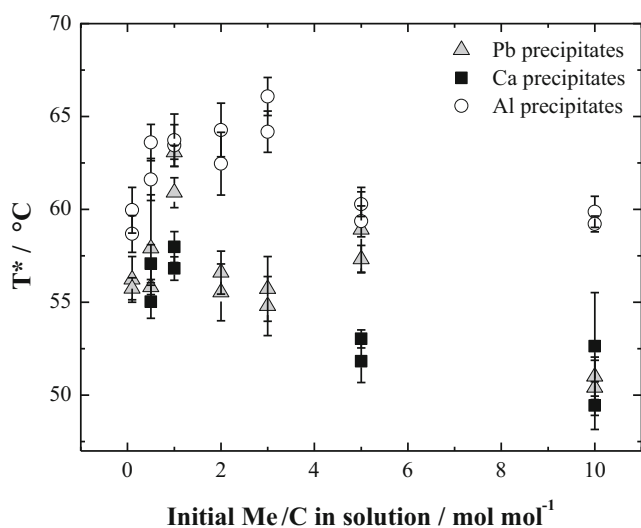


Fig. 2 WaMB transition temperature T^* in dependence of the initial Me/C ratio in solution. Error bars represent standard deviation of measurements

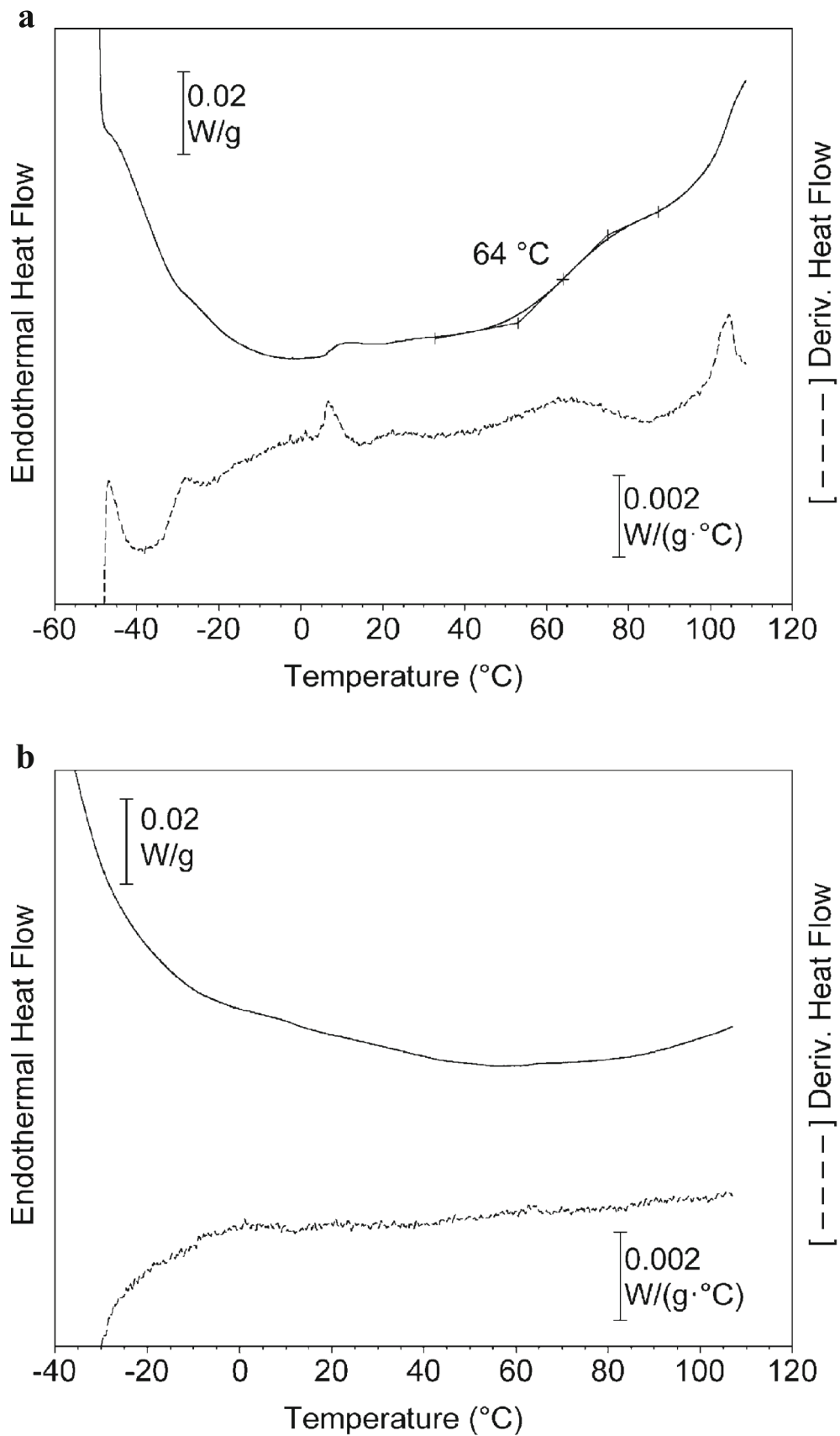
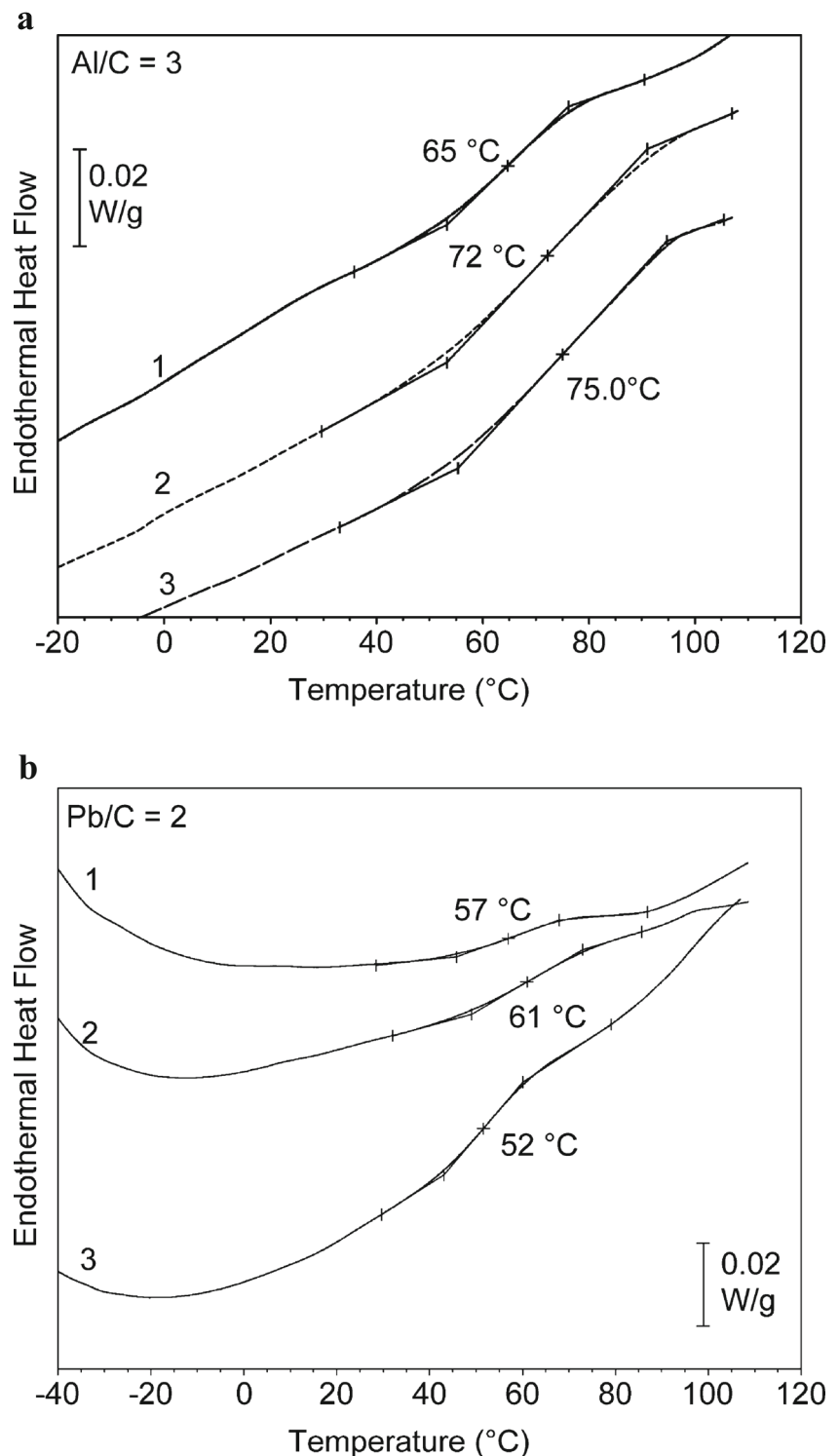


Fig. 3 DSC thermograms (*solid*) and their derivatives (*dashed*) of a representative Al precipitate (Al/C ratio in the initial solution=1) before (a) and after (b) complete water removal at 105 °C

Fig. 4 Heating curves of **a** Pb precipitates (Pb/C ratio in the initial solution=2) and **b** Al precipitates (Al/C ratio in the initial solution=3) measured after 2 weeks of conditioning, after 6 weeks after the first measurement and after 2 weeks after the second measurement



line with the antiplasticisation function of water (Schaumann and LeBoeuf 2005). The Me/C ratio in the precipitates likely has an important impact on matrix rigidity. This is confirmed by the increase in T^* with increasing Al/C ratio in the Al-DOM precipitates derived from the initial solutions with low Al/C ratios which did not differ in water content. Thus, we conclude that intermediate contents of Al in organic

precipitates induce a high degree of cross-linkage in the organic matrix. A comparable increase in rigidity with increasing Ca/C ratio in the precipitate was observed for the Ca precipitates, however at a much lower level. The low T^* observed for all samples precipitated from the initial solutions with a Me/C ratio of 10, suggests that the precipitates formed under large Me/C ratios are less stable and less cross-linked

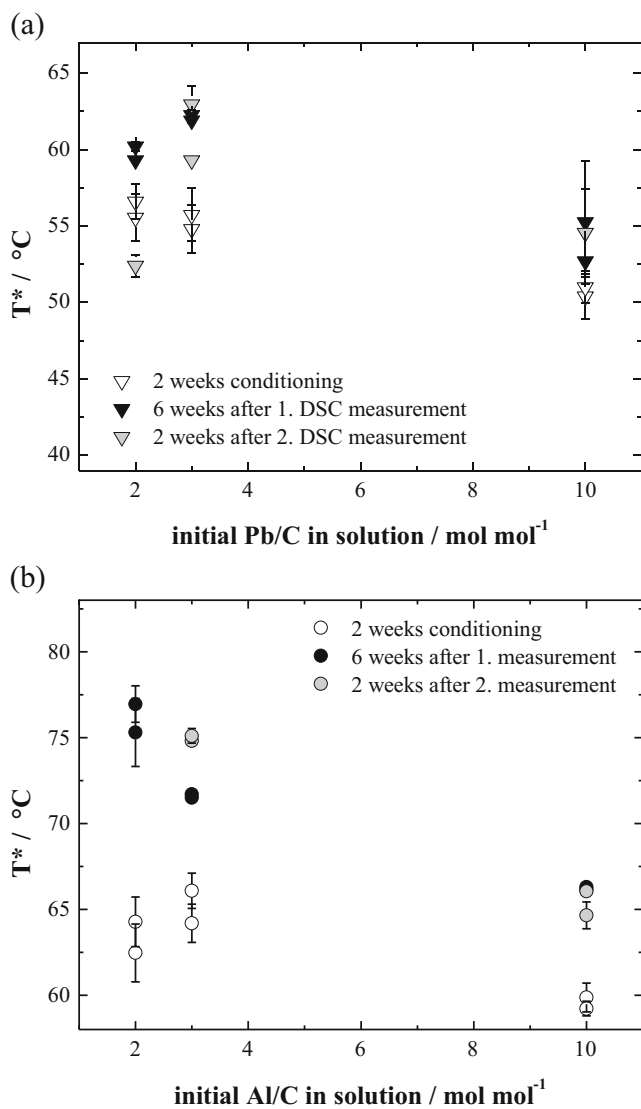


Fig. 5 T^* for **a** Pb precipitates created in solutions with different initial Pb/C ratios and **b** for Al precipitates created in solutions with different initial Al/C ratios. Both variants measured after 2 weeks of conditioning and re-measured 6 weeks after the first and 2 weeks after the second DSC measurement

compared with those formed at lower initial Me/C ratios of the solution. This is further supported by the increase in unprecipitated DOC with increasing Al/C ratios for Al/C above 2, which indicates a reduced DOM binding of Al at high Al concentration (Fig. 1a). Latter would suggest that the precipitates contain a higher portion of multinuclear Al-DOM complexes.

3.2.2 Ageing of Me-DOM precipitates

The WaMB transition is a slowly reversing thermal event that disappears in a directly following second heating cycle, but reappears after some days of sample storage (Schaumann and LeBoeuf 2005). This effect is related to the kinetically retained

reorganisation of the water molecules in the organic matrix. Therefore, the observation of physicochemical ageing (Kunhi Mouvenchery et al. 2013; Schaumann 2006; Schaumann et al. 2013b) is a further support for the assumption that water molecules stabilise the Me-DOM precipitates. Hence, we tested if the thermal event in the Me-DOM precipitates observed during the first heating cycle of the DSC measurements of the water containing precipitates re-appeared after 6 weeks of storage of the samples and after a second storage of 2 weeks after this repeated DSC campaign. These repeated measurements were only conducted for Al and Pb precipitates with Me^{n+}/C ratios of 2 to 10 in the initial solution due to the limited amount of available Ca precipitates.

Generally, the WaMB transition re-appeared after both storage periods (Fig. 4), which is in line with literature (Hurrass and Schaumann 2005; Schaumann and LeBoeuf 2005) observed for peat and soil samples. For Pb precipitates, T^* values of the second measurement were ~ 5 °C higher than for the first (Fig. 4a) demonstrating that a time period of 6 weeks was sufficient for a significant reorganisation of the WaMB within the precipitate matrix. Contrarily, T^* observed after only 2 weeks of storage was markedly lower for Pb/C ratio up to 2 (Fig. 5a). Referring to the WaMB model, this indicates that not all water molecules were reorganised in the organic matrix after only 14 days of equilibration.

The heating curves of the Al precipitates created in a solution with an initial Al/C ratio of 3 exhibited a considerable shift of T^* to higher temperatures (Fig. 4b) for the second and third measurement. In most Al-DOM precipitates, T^* of the third experiments was below that of the second measurement, and in all cases it was larger than that of the first measurement (Fig. 5b). Thus, according to the WaMB model, the water molecules in the Al-DOM precipitates reorganised within a relatively short period after each DSC measurement resulting in a more rigid matrix than due to the equilibrium period before, and it cannot be excluded that the second heating may not have disrupted all WaMB.

4 Conclusions

In summary, our results demonstrate a very similar thermal behaviour of OM bound in precipitates compared with OM in soil samples. The WaMB transition obtained for the DOM precipitates was in the same temperature range obtained for soil samples independently of the initial Me/C ratio of the solution used for the precipitation experiments. This shows that the induced cation-OM bindings present in cation-DOM precipitates are comparable to those in undisturbed soil samples with respect to their thermal behaviour. Precipitates formed with Al and Pb are characterised by a high stability / rigidity of the formed cation-DOM matrix and both cations are good cross-linking agents.

An important outcome of our study is that high cation concentrations do not automatically induce high DOM precipitation ratios. By contrast, large Al concentrations can reduce DOM precipitation, a fact that should be considered especially with respect to the translocation of toxic cations like Pb^{2+} and Al^{3+} in soil in colloidal and/or soluble form. This could be a result of formation of very small and stable AlOOH colloids as indicated by the Al oversaturation in these solutions expected from the speciation modelling. Similar processes have to be expected for other cations relevant in soils like Fe and manganese (Mn), which reveal high affinity to OM and are present in multiple inorganic and organomineral species in soil solution. These colloids possibly catch organic molecules out of the solution and consequently reduce DOM precipitation by this. The measurements furthermore demonstrate the important role of water molecules in rigidity measurements of natural OM. No signals were obtained for water-free precipitates. Based on these results, we conclude that there is a direct connection between water molecules and cations within the formed organic network which cannot be separated from each other. Due to the similarity of the characteristics of the findings in this study to those for solid SOM, it can be hypothesised that similar structures contribute to cross-linking in DOM precipitates as in solid SOM, where combined NMR and DSC studies suggest associations of cation bridges and WaMB relevant for intermolecular cross-linking (Jäger et al. 2011; Kunhi Mouvenchery et al. 2013; Schaumann and Bertmer 2008; Schaumann et al. 2013a, b).

Further studies should investigate the effect of pH and the question to which extent the findings can be transferred to further soil relevant cations including Fe, Mn and Mg and verify the hypothesised WaMB and cation bridge—WaMB structures by additional independent methods. For this, significant method development in NMR, (E)XAFS or SAXS will be highly helpful.

Acknowledgements This study was financially supported by the Deutsche Forschungsgemeinschaft (DFG), project SCHA849/6. We further acknowledge the help of Petra Ziegler, group of Sören Thiele-Bruhn, University Trier, for the measurement of the Al concentrations.

References

- Aquino AJA, Tunega D, Schaumann GE, Haberhauer G, Gerzabek MH, Lischka H (2011) The functionality of cation bridges for binding polar groups in soil aggregates. *Int J Quantum Chem* 111:1531–1542
- Baldock JA, Skjemstad JO (2000) Role of the soil matrix and minerals in protecting natural organic materials against biological attack. *Org Geochem* 31:697–710
- Bardy M et al (2007) Al speciation in tropical podzols of the upper Amazon basin: a solid-state Al-27 MAS and MQMAS NMR study. *Geochim Cosmochim Acta* 71:3211–3222
- Borggaard OK, Raben-Lange B, Gimsing AL, Strobel BW (2005) Influence of humic substances on phosphate adsorption by aluminium and iron oxides. *Geoderma* 127:270–279
- Cao XD, Ma LQ, Chen M, Hardison DW, Harris WG (2003) Weathering of lead bullets and their environmental effects at outdoor shooting ranges. *J Environ Qual* 32:526–534
- Diehl D, Ellerbrock RH, Schaumann GE (2009) DRIFT-spectroscopy of untreated and dried soil samples of different wettability. *Eur J Soil Sci* 60:557–566
- Dudal Y, Holgado R, Maestri G, Guillon E, Dupont L (2006) Rapid screening of DOM's metal-binding ability using a fluorescence-based microplate assay. *Sci Total Environ* 354:286–291
- Gustaffson JP (2010) Visual MINTEQ, version 3.0. <http://www.lwr.kth.se/English/Oursoftware/vminteq/index.htm>. Accessed 08 January 2014
- Hurrass J, Schaumann GE (2005) Is glassiness a common characteristic of soil organic matter? *Environ Sci Technol* 39:9534–9540
- Hurraß J, Schaumann GE (2006) Properties of soil organic matter and aqueous extracts of actually water repellent and wettable soil samples. *Geoderma* 132:222–239
- Jäger A, Schaumann GE, Bertmer M (2011) Optimized NMR spectroscopic strategy to characterize water dynamics in soil samples. *Org Geochem* 42:917–925
- Kalbitz K, Kaiser K (2008) Contribution of dissolved organic matter to carbon storage in forest mineral soils. *J Plant Nutr Soil Sci Z Pflanzenernähr Bodenkunde* 171:52–60
- Khare N, Hesterberg D, Martin JD (2005) XANES investigation of phosphate sorption in single and binary systems of iron and aluminium oxide minerals. *Environ Sci Technol* 39:2152–2160
- Klitzke S, Lang F, Kaupenjohann M (2008) Increasing pH releases colloidal lead in a highly contaminated forest soil. *Eur J Soil Sci* 59:265–273
- Kunhi Mouvenchery Y, Kučerík J, Diehl D, Schaumann GE (2012) Cation-mediated cross-linking in natural organic matter—a review. *Rev Environ Sci Biotechnol* 11:41–54
- Kunhi Mouvenchery Y, Jaeger A, Aquino AJA, Tunega D, Diehl D, Bertmer M, Schaumann GE (2013) Restructuring of a peat in interaction with multivalent cations: effect of cation type and aging time. *PLoS ONE* 8:e65359
- Lang F, Egger H, Kaupenjohann M (2005) Size and shape of lead-organic associations. *Colloid Surf A* 265:95–103
- LeBoeuf EJ, Weber WJ (2000) Macromolecular characteristics of natural organic matter. 1. Insights from glass transition and enthalpic relaxation behavior. *Environ Sci Technol* 34:3623–3631
- Lu YF, Allen HE (2002) Characterization of copper complexation with natural dissolved organic matter (DOM)—link to acidic moieties of DOM and competition by Ca and Mg. *Water Res* 36:5083–5101
- Miikki V, Senesi N, Hanninen K (1997) Characterization of humic material formed by composting of domestic and industrial biowastes. 2. Spectroscopic evaluation of humic acid structures. *Chemosphere* 34:1639–1651
- Mulder J, De Wit HA, Boonen HWJ, Bakken LR (2001) Increased levels of aluminium in forest soils: effects on the stores of soil organic carbon. *Water Air Soil Pollut* 130:989–994
- Oste LA, Temminghoff EJM, Riemsdijk WH (2002) Solid-solution partitioning of organic matter in soils as influenced by an increase in pH or Ca concentration. *Environ Sci Technol* 36:208–214
- Piccolo A (2002) The supramolecular structure of humic substances: a novel understanding of humus chemistry and implications in soil science. *Adv Agron* 75:57–134
- Plaschke M, Rothe J, Denecke MA, Fanghanel T (2004) Soft X-ray spectromicroscopy of humic acid europium(III) complexation by comparison to model substances. *J Electron Spectrosc Relat Phenom* 135:53–62

- Plaschke M, Rothe J, Armbruster MK, Denecke MA, Naber A, Geckeis H (2010) Humic acid metal cation interaction studied by spectromicroscopy techniques in combination with quantum chemical calculations. *J Synchrotron Radiat* 17:158–165
- Römckens P, Dolfing J (1998) Effect of Ca on the solubility and molecular size distribution of DOC and Cu binding in soil solution samples. *Environ Sci Technol* 32:363–369
- Schaumann GE (2005) Matrix relaxation and change of water state during hydration of peat. *Colloid Surf A* 265:163–170
- Schaumann GE (2006) Soil organic matter beyond molecular structure. 2. Amorphous nature and physical aging. *J Plant Nutr Soil Sci* 169:157–167
- Schaumann GE, Bertmer M (2008) Do water molecules bridge soil organic matter molecule segments? *Eur J Soil Sci* 59:423–429
- Schaumann GE, Bertmer M (2013) Soil-water interactions. *eMagRes* 2:493–502
- Schaumann GE, LeBoeuf EJ (2005) Glass transitions in peat—their relevance and the impact of water. *Environ Sci Technol* 39:800–806
- Schaumann GE, Thiele-Bruhn S (2011) Molecular modelling of soil organic matter: squaring the circle? *Geoderma* 169:55–68
- Schaumann GE, Siewert C, Marschner B (2000) Kinetics of the release of dissolved organic matter (DOM) from air-dried and pre-moistened soil material. *J Plant Nutr Soil Sci* 163:1–5
- Schaumann GE, Diehl D, Bertmer M, Jaeger A, Conte P, Alonzo G, Bachmann J (2013a) Combined proton NMR wide-line and NMR relaxometry to study SOM-water interactions of cation-treated soils. *J Hydrol Hydromech* 61:50–63
- Schaumann GE, Gildemeister D, Kunhi Mouvenchery Y, Spielvogel S, Diehl D (2013b) Interactions between cations and water molecule bridges in soil organic matter. *J Soils Sediments* 13:1579–1588
- Scheel T, Dorfler C, Kalbitz K (2007) Precipitation of dissolved organic matter by aluminum stabilizes carbon in acidic forest soils. *Soil Sci Soc Am J* 71:64–74
- Scheel T, Haumaier L, Ellerbrock RH, Ruhlmann J, Kalbitz K (2008) Properties of organic matter precipitated from acidic forest soil solutions. *Org Geochem* 39:1439–1453
- Schwesig D, Kalbitz K, Matzner E (2003) Effects of aluminium on the mineralization of dissolved organic carbon derived from forest floors. *Eur J Soil Sci* 54:311–322
- Shen YH (1999) Sorption of humic acid to soil: the role of soil mineral composition. *Chemosphere* 38:2489–2499
- Weng LP, Temminghoff EJM, Lofts S, Tipping E, Van Riemsdijk WH (2002) Complexation with dissolved organic matter and solubility control of heavy metals in a sandy soil. *Environ Sci Technol* 36:4804–4810
- Wershaw RL (2004) Evaluation of conceptual models of natural organic matter (Humus) from a consideration of the chemical and biochemical processes of humification U.S. Department of the Interior, U.S. Geological Survey Reston, Virginia
- Xia K, Bleam W, Helmke PA (1997) Studies of the nature of binding sites of first row transition elements bound to aquatic and soil humic substances using X-ray absorption spectroscopy. *Geochim Cosmochim Acta* 61:2223–2235